

RESEARCH ARTICLE



MAGNETIC & STRUCTURAL PROPERTIES OF Ce³⁺ SUBSTITUTED Ni-Zn NANOFERRITES SYNTHESIZED IN SOL-GEL METHOD

THUMMAPUDI NIRANJAN KUMAR¹, CH. VIJAY ANIL DAI² K.SURESH³

¹Lecture in physics, AMAL College Anakapalli, Visakhapatnam, Andhra Pradesh

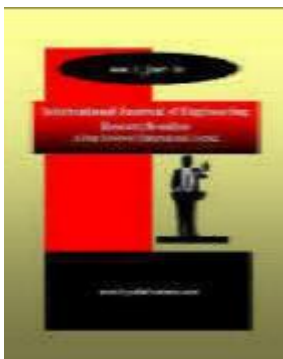
²Lecture in physics, A.G & S.G Siddhartha College of Arts and Science, Vuyyuru, Krishna, A.P

³Lecture in Physics, VSR & NVR Degree College, Tenali, Guntur Dist., A.P., India

Article Received: 11/12/2013

Article Revised: 20/1/2014

Article Accepted: 06/02/2014



ABSTRACT

Cerium substituted nickel–zinc ferrite with general formula Ni_{0.2} Zn_{0.4} Ce_x Fe_{2-x}O₄ (where x=0.0, 0.1, 0.2, 0.3) were synthesized by synthesized via co-precipitation of metal hydroxides, followed by calcinations. The obtained powder was sintered at 1000°C for 2h. The detailed structural and magnetic studies were carried out through X-ray diffraction (XRD), Fourier transform infrared spectroscopy (FTIR), and scanning electron microscope (SEM). The XRD pattern of as prepared sample confirms the formation of single phase with cubic spinel structure. The average crystallite size was found to be 22 to 34 nm and decreases with increasing Ce³⁺ ion concentration. The IR spectra exhibited two expected absorption bands between 600 to 400 cm⁻¹ corresponding to the stretching vibrations of tetrahedral (A) and octahedral (B) metal oxygen vibrations. Their crystal structure was characterized via X-ray diffraction analysis, confirming that the Ce-substituted Ni-Zn ferrite samples had a single-phase spinel structure. The metal composition significantly affected the crystal structure, including the lattice parameters and crystallite size. The magnetic properties of the samples exhibit a strong dependence on the phase composition, particle size and preparation method. The hysteresis loop confirms the magnetic behaviour of the prepared composition, which is then discussed on the basis of cation distribution. The parameters such as saturation magnetization, coercivity, and retentivity are calculated. The Curie temperature was found to decrease with increasing Ce³⁺ content.

©KY PUBLICATIONS

Introduction

The mixed spinel nano-ferrites have a wide range of applications in the various fields of science and technology. Various ferrite preparation techniques, doping and cation substitutions play an extraordinary role in deciding and controlling the characteristics of nanoferrite particles. Substituting the trivalent and pentavalent ions gives rise to many applications of ferrites in different areas such as magnetic storage,

transformer cores, magnetic cards, magnetic recording, permanent magnets, computer peripherals, electronic devices, microwave devices and catalysts¹. Complex synthesis process and lower production rate are the main problems of wet-chemical methods². Sol-gel auto-combustion or auto-ignition preparation method where the chemical sol-gel and ignition process is combined, this powder preparation showed great possibility in the synthesis of spinel type ferrite nanomaterials. This method of synthesis can be considered as solution combustion technique³. It has been applicable for the preparation of different spinel ferrite compounds MFe_2O_4 , where M could be Zn, Ni, Co, Cu, Mg, Mn ion or its combination⁴. Normally, in ferrites nickel has a strong tendency to occupy the octahedral sites whereas zinc occupies the tetrahedral site. Thus, nickel ferrite has an inverse spinel structure whereas zinc ferrite has a normal spinel structure. Hence, Ni-Zn ferrites have a mixed spinel ferrite structure and are used as a wave absorber for electromagnetic interference⁵. There are two main classes of materials containing zinc ferrites, that is, Mn-Zn ferrites and Ni-Zn ferrites. Out of them Ni-Zn ferrites are designed for very high frequency operation, to more than 100 MHz as well as very high resistivity, about 10^5 ohm cm. Several studies have focused on the variation of Ni-Zn ferrite microstructure by changing the Zn or Ni content and sintering conditions⁶

The magnetic and electrical properties of the nano ferrites are affected by the preparation conditions, chemical composition, sintering temperature and the method of preparation. Several chemical and physical methods such as spray pyrolysis, sol-gel, co-precipitation, combustion technique, high energy milling etc. have been used for the fabrication of stoichiometric and chemically pure nano ferrite materials. Among the available chemical methods, the sol-gel technique is an excellent method to synthesize rare earth substituted nanoparticles with maximum purity. In spite of the development of a variety of synthesis routes, the production of nickel ferrite nanoparticles with desirable size and magnetic properties is still a challenge. This would justify any effort to produce size tuned nickel ferrite nanoparticles with rare earth substitution. In The present work is done to record and analyse structural changes with the help of XRD, FTIR, SEM etc techniques by the Ce^{3+} substituted Ni-Zn ferrite for various Ce^{3+} concentrations at room temperature and liquid nitrogen temperature. This work is a step towards studying the physical processes leading to anomalous behavior of magnetization in the Ce-substituted Ni-Zn ferrites.

Materials and Methods

Synthesis of Nickel ferrites : Nano particles of cerium substituted nickel ferrite were synthesized by the sol-gel combustion method at low temperatures for different compositions $Ni_{0.2} Zn_{0.4} Ce_x Fe_{(2-x)} O_4$ (where $x=0.0, 0.1, 0.2, 0.3$). Raw materials are used in the experiments are AR grade nitrates i.e. $Ni(NO_3)_2 \cdot 6 H_2O$, $Ce(NO_3)_3 \cdot 6 H_2O$, $Fe(NO_3)_3 \cdot 9 H_2O$ (GR) in their respective stoichiometry and citric acid monohydrate - $C_6H_8O_7 \cdot H_2O$ (GR) is used as a fuel in the ratio 1:3, all from Merck company of purity of 99 % using stoichiometric ratio and dissolved in distilled water. The mixture of the raw material was stirred till to get the homogeneous solution then maintaining pH 7.0 by adding ammonia. After at $80^\circ C$ on hot plate magnetostirrer, it was continuously stirred to obtain uniform gel. After 6 hours it converts from gel to ash form, which was sintered at $800^\circ C$. The resultant powder was then ground into fine particles by an agate mortar and pestle

Structural characterization

X-Ray Diffraction (XRD): X-ray diffraction is now a common technique for the study of crystal structures and atomic spacing. The patterns for the MnO nanoparticles were recorded using an X-ray diffractometer (PANLYTICAL) using secondary monochromatic Cu $K\alpha$ radiation of wavelength $\lambda = 0.1541$ nm at 40 Kv/50 mA in the scan range $2\theta = 20^\circ$ to 90° . Samples were supported on a glass slide.

Scanning Electron Microscopy (SEM): Morphology of the samples was investigated using scanning electron microscope (model JSM-7000F) which also has been used for compositional analysis of the prepared MnO nanoparticles. A drop of nanoparticles dissolved in methanol was placed on a copper grid.

Fourier Transform Infrared Spectroscopy (FTIR): The fourier transform infrared (FTIR) absorption spectra of the samples were recorded using FTIR spectrometer (Thermo Nicolet, Avatar 370) in the wave number range $4000-400$ cm^{-1} with Potassium bromide (KBr) as binder.

The magnetic characterization was carried out using a Vibrating Sample Magnetometer (VSM; Lakeshore 7410) at room temperature up to a maximum field of 20 kOe.

XRD studies

The structural analysis of $\text{Ni}_{0.2}\text{Zn}_{0.4}\text{Ce}_x\text{Fe}_{2-x}\text{O}_4$ (where $x=0.0, 0.1, 0.2, 0.3$) ferrite nanoparticles calcined at 800 °C was performed by powder XRD method. Figure 1 shows the X-ray diffraction patterns of all prepared ferrite nanoparticles and confirm their crystalline structure with single phase spinel phase. The average crystallite size of the ferrite nanoparticles was calculated using the Debye-Scherrer equation⁷:

$$t = \frac{0.9\lambda}{\beta \cos \theta}$$

Where, λ is wavelength of the X-ray radiation, is full width at half maximum, β is Bragg's angle. It was found that the average crystallite size of the ferrite nanoparticles is in the range 17 to 24 nm. It was noticed that the crystallite size and lattice constant gradually decreased with increasing Ce^{3+} ion concentration (Table 1). Decrease in the crystallite size and lattice constant may be due to the substitution of larger Zn^{2+} ions (0.84 Å) with smaller Ce^{3+} ions⁸. The average crystallites size (D), the degree of microstrain (e), and the lattice parameter (a) of the studied nickel-zinc ferrites are also determined from the experimental XRD profiles (Table 1) by using the Williamson-Hall analysis. A well defined effect of the crystals size decrease and increase in the crystal defects and lattice parameter is observed for the mechanochemically obtained materials (Table 1). A dependence of the lattice parameter on the preparation method and the phase composition exists.

Table 1: Structural parameters of samples cerium substituted nickel ferrites

Sample	Peak position	FWHM (Å)	Crystallite size (D) (nm)	Strain (e)	Interplanar Spacing d (Å)	Lattice parameter (a)
$\text{Ni}_{0.2}\text{Zn}_{0.4}\text{Ce}_x\text{Fe}_2\text{O}_4$ ($x=0.0$)	35.49	0.50	23.11(±1.4)	0.0071	2.6265	8.7149
$\text{Ni}_{0.2}\text{Zn}_{0.4}\text{Ce}_{0.1}\text{Fe}_{1.9}\text{O}_4$ ($x=0.1$)	35.66	0.46	20.91(±0.9)	0.0063	2.6154	8.6742
$\text{Ni}_{0.2}\text{Zn}_{0.4}\text{Ce}_{0.2}\text{Fe}_{1.8}\text{O}_4$ ($x=0.2$)	35.73	0.43	19.73(±1.6)	0.0067	2.6134	8.6677
$\text{Ni}_{0.2}\text{Zn}_{0.4}\text{Ce}_{0.3}\text{Fe}_{1.7}\text{O}_4$ ($x=0.3$)	35.80	0.39	17.75 (±1.2)	0.0061	2.6022	8.6305

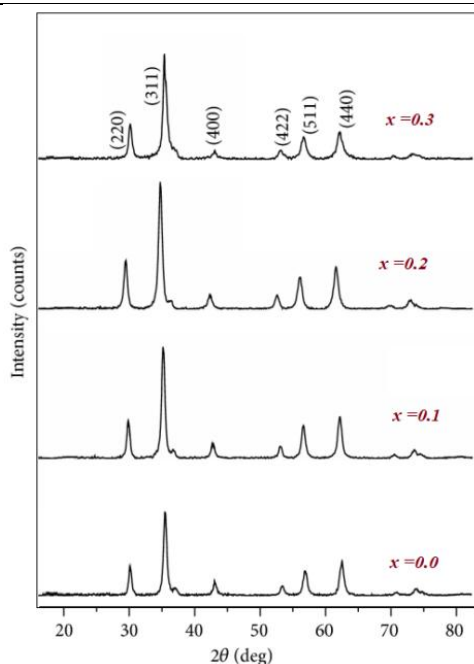


Figure 1: X-ray diffraction patterns for $\text{Ni}_{0.2}\text{Zn}_{0.4}\text{Ce}_x\text{Fe}_{2-x}\text{O}_4$ (where $x=0.0, 0.1, 0.2, 0.3$)

FTIR study

The FTIR spectra for $\text{Ni}_{0.2}\text{Zn}_{0.4}\text{Ce}_x\text{Fe}_{2-x}\text{O}_4$ (where $x=0.0, 0.1, 0.2, 0.3$) are shown in Figure 2. By overlaying the FTIR spectra for Fe_2O_3 and for $\text{Ni}_{0.2}\text{Zn}_{0.4}\text{Ce}_x\text{Fe}_{2-x}\text{O}_4$ with $x = 0, 0.1, 0.2, \& 0.3$, the spectral similarities are

observed. The broad feature between $3441.43 - 3219.90 \text{ cm}^{-1}$ is due to O-H stretch which corresponds to the hydroxyl groups attached by the hydrogen bonds to the iron oxide surface and the water molecules chemically adsorbed to the magnetic particle surface⁹. From these results, it appears that the hydroxyl groups are retained in the samples during the preparation of the uncoated Ni-Zn Fe_2O_4 spinel ferrites prepared by sol-gel methods. The FT-IR spectra of all the present samples show two IR characteristics bands between 420 and 600 cm^{-1} which are attributed to the Fe-O stretching vibration of ferrite materials¹⁰. A minor broad IR band seen at $\sim 3480 \text{ cm}^{-1}$ in all the samples is due to O-H stretching band of H_2O ¹¹.

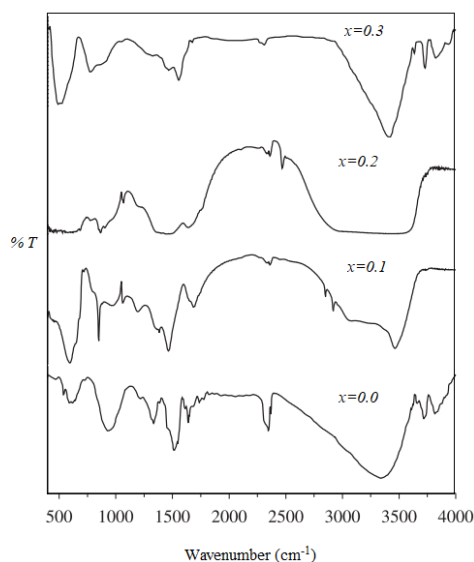


Figure 2: FT IR Spectra of $\text{Ni}_{0.2}\text{Zn}_{0.4}\text{Ce}_x\text{Fe}_{2-x}\text{O}_4$ (where $x=0.0, 0.1, 0.2, 0.3$)

Scanning Electron Microscopy (SEM) study: Figures 3 show typical scanning electron microscopic (SEM) images of $\text{Ni}_{0.2}\text{Zn}_{0.4}\text{Ce}_x\text{Fe}_{2-x}\text{O}_4$ (where $x=0.0, 0.1, 0.2, 0.3$) respectively. It is clear from these electron micrographs that the material essentially consists of some irregularly cubic particles in pure Ni-ferrite. Well-crystallized dense grains of irregular shapes were observed for these compositions with the presence of large micropores. The continuous decrease in grain size with Ca substitution may be due to the fact that Ce^{3+} ions have large ionic radii than that of Fe^{3+} (0.64 \AA) and, therefore, show limited solubility in spinel lattice and prevent grain growth resulting in decrease in grain size¹².

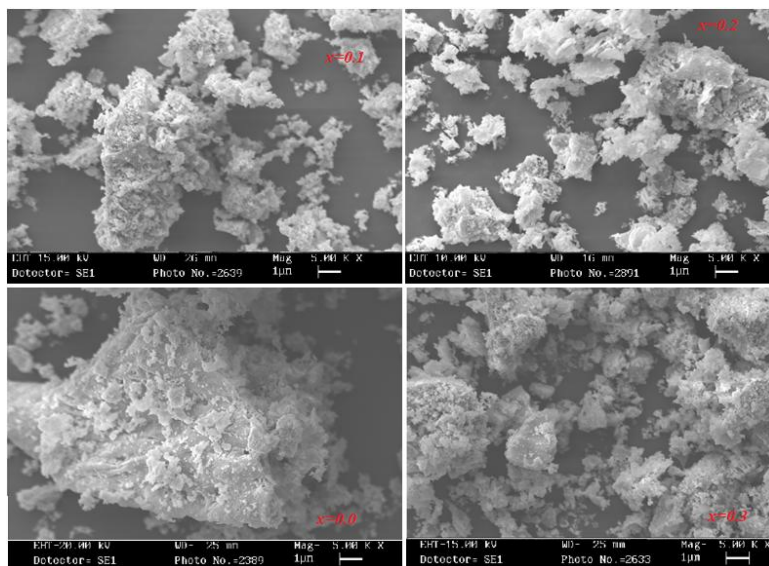


Figure 3: Scanning electron microscopic (SEM) photographs of $\text{Ni}_{0.2}\text{Zn}_{0.4}\text{Ce}_x\text{Fe}_{2-x}\text{O}_4$ (where $x=0.0, 0.1, 0.2, 0.3$) ferrite

Magnetic properties

Figure 3 shows the magnetic properties of the synthesis samples, it shows that the compositions of Ce^{3+} contain increase the H_c (Coercivity) , M_r (Magnetic remanence) and M_s (Magnetic saturation) all are decreasing. To study the effects of Ce^{3+} doping on magnetization, coercivity, remanent magnetization (M_r) and magneto-crystalline anisotropy (HK) of Ni-Zn-Fe, M-H hysteresis loops were recorded using VSM under the applied magnetic field of 10 kOe at room temperature. Figure 3 shows the hysteresis curves for all the samples under investigation. It is clear that all the samples show a fine s shape loops with a decrease in magnetization (M_s) and coercivity (H_c) with increase in Ce^{3+} concentration. This is due to the substitution of Ce^{3+} in place of Fe^{3+} at B-sites. The order in magnetic moments of rare earth ions is below room temperature; due to this at room temperature Ce^{3+} ion behaves as non magnetic that causes a decrease in saturation magnetization and coercivity. This substitution causes a lattice distortion that alters the magnetic characteristics of materials. Magnetic properties of ferrite materials largely based upon the grain size, cation substitution, and A-B exchange interactions. Increase in the grain size and decrease of A-B super exchange interaction causes canting spins at the surface of nano particles that decreases the magnetic characteristics of the present samples. Spin arrangement for the Ni-Ce-Zn ferrites were analyzed by measuring the value of Bohr's magnetron by the relation

$$n_B = \frac{\sigma_s}{5585} M_W$$

Where $n_B = (6 + x) \cos \alpha_{Y-K} - 5(1 - x)$

where x represents the composition of doping ion. anisotropy field (H_k) can be calculated by following equations

$$H_k = \frac{2K_1}{\mu_0 M_s}$$

where μ_0 is the permeability of the free space, M_s is saturation magnetization from the fit. It is clear from the data that cubic anisotropy decreases with increase in Cerium concentration. Pure nickel ferrite is has high anisotropy constant and field due to occupation at B-sites. The anisotropy parameters (anisotropy constant and field) are not decreasing monotonically but more abruptly due to differing concentration of doping ion. This behaviour is showing a strong lattice distortion due to Ce^{3+} substitution. Nano spinel $\text{Ni}_{0.2}\text{-Ce}_x\text{-Zn}_{0.4}\text{-Fe}_{2-x}\text{O}_4$ with x in step increment of 0.1 has been synthesized by sol-gel combustion. All the studied samples are pure cubic spinel phase ferrites without any impurity metal oxides. Magnetic anisotropy of nickel-ferrite nano particles decreases with increase in Ce^{3+} concentration (x). Thus the rare earth (Ce^{3+}) doped nickel-ferrites found an application in high frequency devices and power supply due to high resistivity and low losses.

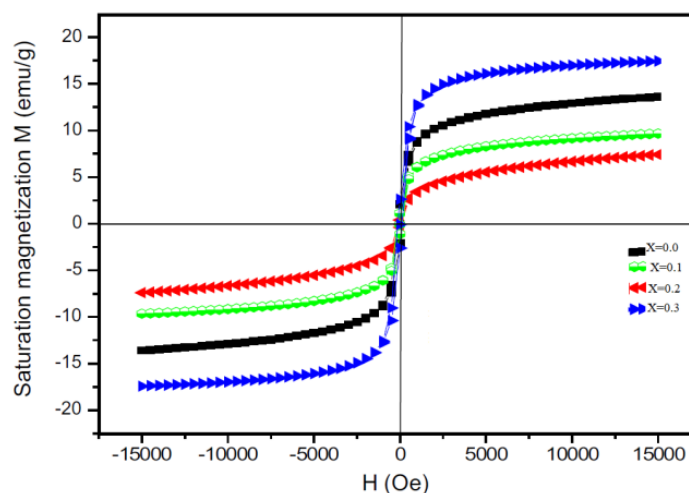


Figure 4. M-H loops of $\text{Ni}_{0.2}\text{Zn}_{0.4}\text{Ce}_x\text{Fe}_{2-x}\text{O}_4$ (where $x=0.0, 0.1, 0.2, 0.3$) ferrite nanoparticles

Conclusion

We successfully synthesized and characterized the $\text{Ni}_{0.2}\text{Zn}_{0.4}\text{Ce}_x\text{Fe}_{2-x}\text{O}_4$ (where $x=0.0, 0.1, 0.2, 0.3$) ferrite nanoparticles using sol-gel technique. XRD and the FTIR pattern showed that all the compositions were formed into single phase cubic spinel structure. The lattice parameters and the grain size were found decreasing with Ce^{3+} content. The SEM images showed the crystalline structure where as EDX patterns confirmed the compositional formation of the synthesized samples. It is observed that particle size is decreased with the Ce^{3+} content. Magnetic studies by Vibrating Sample Magnetometer (VSM) shows that magnetization (Ms) decreases with increase in Ce^{3+} concentration.

References

- 1 S. Sharma, K. Verma, U. Chaubey, V. Singh, B.R. Mehta, "Influence of Zn substitution on structural, micro structural and dielectric properties of nanocrystalline nickel ferrites", Mater. Sci. Eng. B, 167 (2010) 187–192
- 2 Sarangi, P.P.; Vadera, S. R.; Patra, M K; Powder Technology 2010, 203, 348–353
- 3 Aruna, S T; Mukasyan, .A. S.; *Current Opinion in Solid State and Mat. Sci.* 2008, 12, 44–50.
- 4 Sutka, A.; Mezinskis, G.; Pludons, A.; Power Engi. 2010, 56, 254–259.
- 5 S.B. Waje, M. Hashim, W.D.W. Yusoff, Z. Abbas, "Sintering temperature dependence of room temperature magnetic and dielectric properties of $\text{Co}_{0.5}\text{Zn}_{0.5}\text{Fe}_2\text{O}_4$ prepared using mechanically alloyed nanoparticles", J.Magn.Magn.Mater., 322 [6] (2010) 686–691
- 6 T. J. Shindea, A. B. Gadkari, and P. N. Vasambekar, "DC resistivity of Ni-Zn ferrites prepared by oxalate precipitation method," Materials Chemistry and Physics, vol. 111, no. 1, pp. 87–91, 2008
- 7 B.D. Cullity, Elements of X-ray Diffraction, 2nd ed. Addison-Wesley, Reading, MA, 1978
- 8 I.H. Gul, W. Ahmed, A. Maqsood, "Electrical and magnetic characterization of nanocrystalline Ni-Zn ferrite synthesis by co-precipitation route", J. Magn. Magn. Mater., 320 [3] (2008) 270–275
- 9 Creanga D and Calugaru G. Physical investigations of a ferrofluid based on hydrocarbons. Journal of Magnetism and Magnetic Materials (Amsterdam). 2005; 289:81-83.
- 10 Jiang J, Ai LH, Liu L-Y (2010) Poly(aniline-co-o-toluidine)/ $\text{BaFe}_{12}\text{O}_{19}$ composite: preparation and characterization. Mater Lett 64:888–890
- 11 Huang J, Zhuang H, Li WL (2003) Synthesis and characterization of nano crystalline $\text{BaFe}_{12}\text{O}_{19}$ powders by low temperature combustion. Mater Res Bull 38:149–159
- 12 C. Kittel, Introduction a La Physique de L'etat Solide, Dunod, Paris, France, 1958.